PNAS RESEARCH ARTICLE | EVOLUTION

Evolution induced state shifts in a long-term microbial community experiment

Mikko Kivikoski[a,b], Johannes Cairns[a,b,c,d,1], Shane L. Hogle[d], Sanna Pausio[d], Lutz Becks[e], Ville Mustonen[a,b,2,3], and Teppo Hiltunen[d,2,3]

Affiliations are included on p. 8.

Edited by Bruce R. Levin, Emory University, Atlanta, GA; received November 19, 2025; accepted April 21, 2026

Biological communities are complex, dynamic systems that underpin ecosystem functionality, yet their long-term dynamics and predictability remain poorly understood. Understanding how Darwinian evolution shapes these systems through eco-evolutionary feedback is a central challenge in ecology and evolution. Experimental studies using simplified microbial assemblages have yielded important insights into the ecological principles governing community states. However, an important knowledge gap is how selection within member species drives changes of community state in multispecies systems. Here, we present a four-year evolution experiment involving a 23-species synthetic bacterial community propagated in two environments: a control medium and the same medium supplemented with the antibiotic streptomycin. Through combined analyses of community composition and genome evolution, we quantified the temporal changes in species abundances and the evolutionary trajectories of individual community members. The extended duration of the experiment enabled the detection of adaptive mutations and community state shifts that occur only over long evolutionary timescales. We show that community dynamics are environment dependent and reproducible across replicates and that evolution of streptomycin resistance in a previously streptomycin-sensitive species on its own can induce abrupt community state shifts. Our results provide a direct demonstration of eco-evolutionary feedbacks within a multispecies community, revealing how a single adaptive mutation can reorganize complex ecological networks.

eco-evolutionary dynamics | experimental evolution | microbial communities | state shifts

Significance

Ecological communities are complex and dynamic systems and their composition—as well as changes in that—are difficult to predict. This is a major challenge especially with microbes, key players for example in global biogeochemical cycles and human health. In particular, we do not know how evolution affects multispecies communities and how eco-evolutionary feedback potentially alter the community state. To address this question, we analyze community composition and species evolution of a synthetic 23-species bacterial community in a 4-y microcosm study. We show that de novo mutation in a single key community member can alter the ecological state of the whole community, demonstrating eco-evolutionary feedback dynamics in a community context.

The biodiversity around us is an assembly of species that live and interact in communities. The composition of these communities—defined by the identities and abundances of their member species—emerges from assembly processes shaped by environmental conditions and interspecific interactions (1). Classic examples show how environmental change and interactions shift communities, from state changes in lakes (2) to microbiome restructuring after antibiotics (3) Yet it remains unclear whether assembly follows general rules or reflects emergent, context-dependent properties (4, 5).

Evolution adds another layer of complexity, operating alongside ecological assembly to shape community trajectories. Microbes, with their short generation times, are particularly tractable models for studying these dynamics, although short-term studies often miss slower evolutionary changes. The long-term *Escherichia coli* evolution experiment (LTEE) has shown that molecular evolution can persist for more than 60,000 generations, even after fitness increase plateaus (6). These insights have reshaped our understanding of adaptation and spurred theoretical advances such as clonal interference (7) and predictive evolutionary frameworks (8–10). Yet single-species systems capture only part of the picture: Natural communities are far more complex. Ecological processes like species sorting structure community assembly and responses to perturbations (11–15), but how evolution unfolds within these dynamics and feeds back to alter community states remains unresolved. Ecological conditions not only shape community structure but also drive Darwinian evolution, which can cascade back to reorganize entire communities (16). These eco-evolutionary feedbacks represent a key gap in our ability to predict long-term community outcomes (17).

Bridging this gap requires closer integration of population genetics and community ecology (18, 19). Unlike single-species systems, multispecies communities involve direct interactions such as cross-feeding, toxins, and quorum sensing, as well as indirect interactions through shared-resource competition (20). Theory and experiments increasingly show that the fitness effects of mutations depend on community context (21–23), producing evolutionary outcomes that diverge from those in isolated populations (24–28).

Author contributions: M.K., L.B., V.M., and T.H. designed research; M.K. and S.P. performed research; S.L.H. contributed new reagents/analytic tools; M.K. and J.C. analyzed data; M.K., J.C., S.L.H., S.P., L.B., V.M., and T.H. review & editing, funding acquisition, supervision; and M.K., J.C., S.L.H., S.P., L.B., V.M., and T.H. wrote the paper.

The authors declare no competing interest.

This article is a PNAS Direct Submission.

[1]Present address: Department of Experimental Medical Science, SciLifeLab, Lund University, Lund 223 62, Sweden.

[2]V.M. and T.H. contributed equally to this work.

[3]To whom correspondence may be addressed. Email: v.mustonen@helsinki.fi or teppo.hiltunen@utu.fi.

This article contains supporting information online at https://www.pnas.org/lookup/suppl/doi:10.1073/pnas.2533269123/-/DCSupplemental.

Published May 27, 2026.

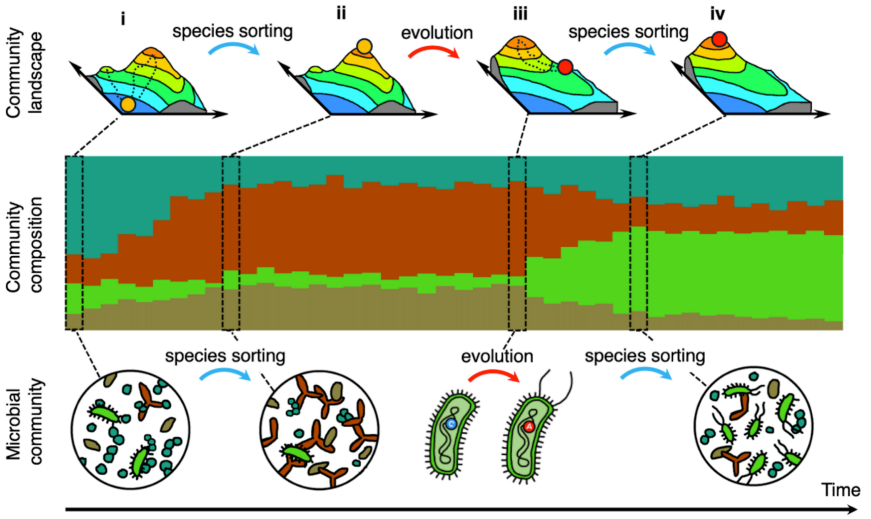

Fig. 1. Microbial community composition, i.e. state, is shaped by ecological interactions, evolution, and their interplay. We studied how microbial communities (*Bottom*) move across the community state space and change over time. The stacked bar chart (*Middle*) shows the relative abundances of the member species (schematic). The *Top* row depicts a schematic, low-dimensional, representation of the underlying high-dimensional dynamical system as a landscape where the microbial community (filled circle) moves due to ecological forces. The community moves typically toward one of the (local) maxima, and the succession path is dictated by the interaction of species with themselves and the environment and affected by stochastic forces such as demographic noise [panel (*i*), dashed lines show example paths leading to different maxima]. If the time-scale is long enough Darwinian evolution could change the dynamical multispecies system. Panel (*iii*) demonstrates such a scenario where, after initial rapid species sorting (*i* → *ii*), a community member species acquires an adaptive mutation which alters the eco-environmental system and its dynamics, seeding a new high-dimensional dynamical system. Such a major event can be followed by fast species sorting dynamics occurring again as the community moves toward a (possible) stable state (*iii* → *iv*). Several, a priori possible dynamical scenarios could occur, and the figure illustrates one such scenario. For example, replicated microbial communities within an environment could go to different states, via different sequences of states, or to the same state via the same or different sequence of states, and these dynamics may or may not be affected by evolution.

Understanding and predicting community dynamics will therefore require approaches that explicitly integrate ecological interactions with evolutionary change across timescales.

Extending long-term evolutionary approaches to multispecies microbial communities can illuminate how molecular evolution within one species triggers cascading effects that shift whole community states. Developing experimental frameworks that connect ecological and evolutionary processes over short and long timescales is a critical step toward predictive community ecology (Fig. 1). Here, we present our findings from the first 210 wk of an ongoing community experiment involving a synthetic 23-species bacterial community. The community is not a subset of any natural community but represents a multispecies community that can be maintained in a species rich state in various laboratory conditions including when manipulated for example with antibiotic stress (12) or predation pressure (24).

We tracked community composition, or the relative abundance of species, and the molecular evolution of member species in two environments differing in the presence of the antibiotic streptomycin. Streptomycin was applied at a concentration of 20 $\mu g \times ml^{-1}$ which is a sublethal concentration for some species in the community while sufficiently high to likely select for resistance in many of the community members (13, 29). Six replicate communities were propagated in each environment. This design enabled us to examine the interaction between species sorting (ecological filtering) and evolutionary change in shaping community dynamics and to test whether molecular evolution influences the stability and trajectories of multispecies communities.

Results

Environment Changed the Community Composition. Study environments, base (B) and streptomycin (S), had a substantial short-term effect on the community composition: The community states diverged markedly between absence and presence of streptomycin (Fig. 2). In both environments, a 32-d long serial transfer experiment, replicated 48 times, revealed rapid and highly repeatable species sorting, consistent with earlier studies, e.g., refs. 30–33. These differences arose from eco-environmental effects, namely, differential sensitivity to streptomycin (*SI Appendix*, Table S1) and the interactions among the species. The most pronounced difference in the community state was the relative abundance of *Aeromonas caviae* and *Citrobacter koseri*: *A. caviae* is sensitive to streptomycin and had the highest relative abundance in the base environment, but negligible abundance in streptomycin, whereas *C. koseri*, which is resistant to streptomycin, showed the opposite pattern.

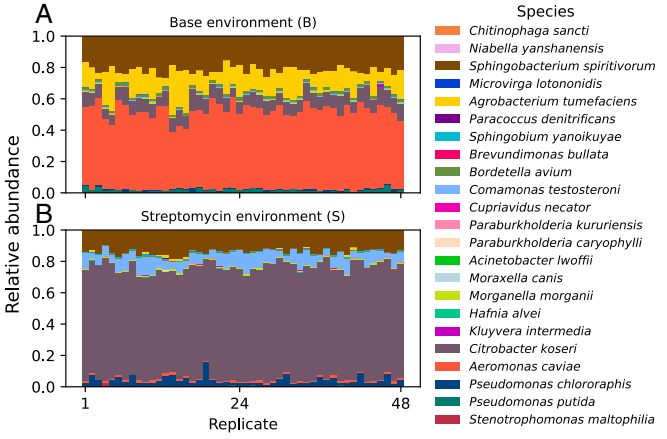

Fig. 2. Community composition differs between base and streptomycin environments. Stacked bar charts show the relative abundances of the 23 species in 48 replicates after 32 d of serial transfer (every 48 h) in (*A*) base and (*B*) streptomycin environments.

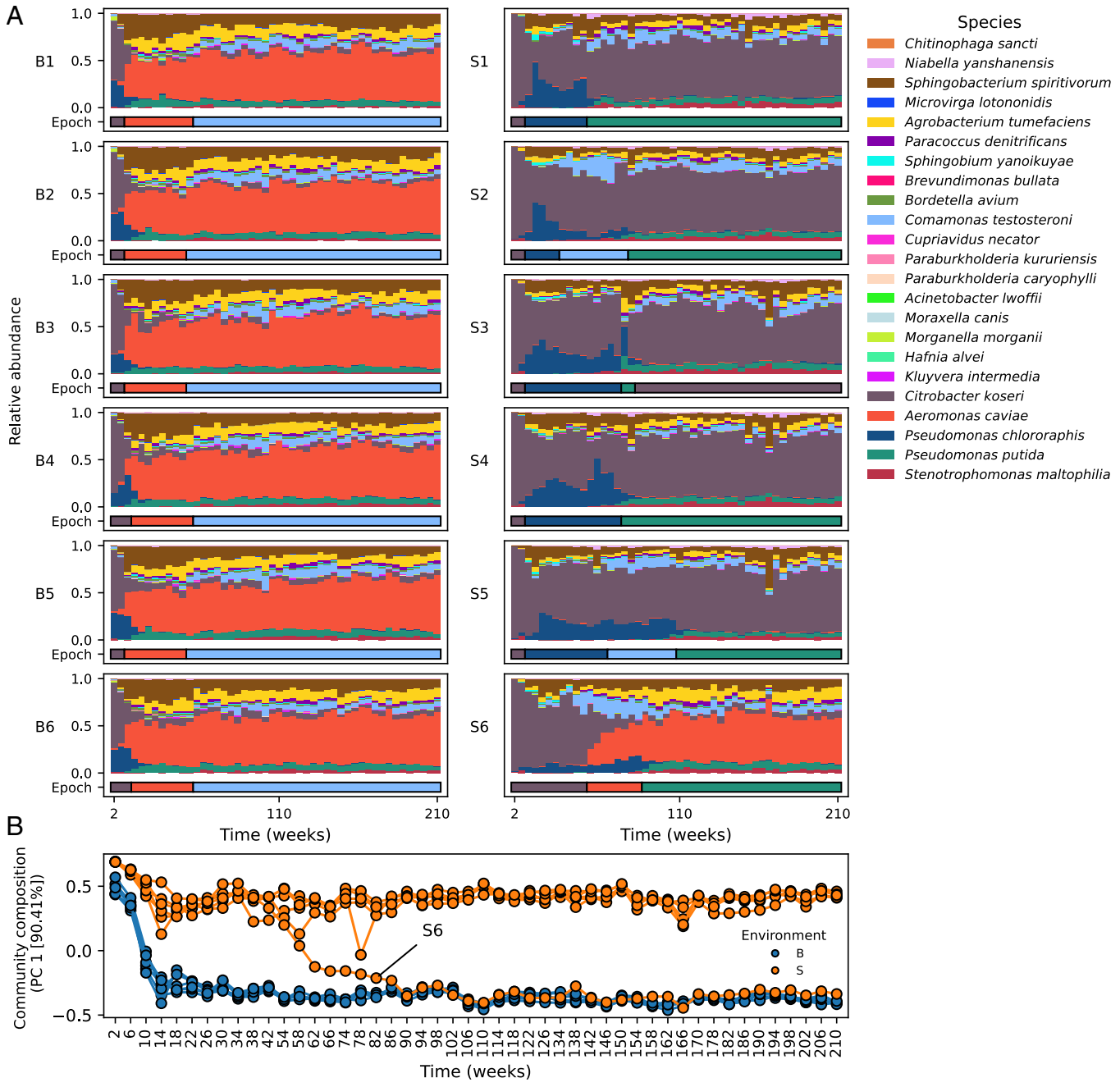

Fig. 3. Community composition over time in six base and streptomycin environment replicates (B1–B6 and S1–S6, respectively). (*A*) Stacked bar charts show the relative abundances of each of the 23 species per time point. Horizontal bars show the epochs (3–4 per replicate) and their break points indicating state shifts. Epoch color indicates the species whose abundance change has the greatest impact on the inference of epoch change and differs from the previous epoch-determining species (*Materials and Methods*). (*B*) Principal component 1 (PC 1) depicts the path of community succession. Each point corresponds to one timepoint in one replicate. Deviation of replicate S6 from the other S communities is highlighted. Percentage of the variance explained by PC 1 is indicated in the label of the y-axis.

Long-Term Experiment Revealed Successive, Repeatable, Community State Shifts. The long-term experiment revealed successive, repeatable, community state transitions and diverging fates across six base and streptomycin environment replicates (B1–B6 and S1–S6, respectively). These dynamics were observed in a 210-wk experiment with 48 longitudinal samples to assess the dynamics of community composition and evolution. The data revealed distinct succession in the two environments (Fig. 3). We segmented the time series into discrete epochs representing succession states. In both environments, except in replicate S6, the initial epoch was brief, representing a rapid transition from the inoculum to an eco-environmental determined state. In the base environment, all six replicates (B1–B6) followed a highly repeatable three-epoch succession pattern (Fig. 3; endpoint repeatability index of 0.97, *SI Appendix*, Fig. S1). In the streptomycin environment, five replicates (S1–S5) converged on a shared succession path (endpoint repeatability index = 0.96, *SI Appendix*, Fig. S1), although the number and timing of the epochs varied (Fig. 3). By contrast, replicate S6 diverged from the other replicates ultimately reaching a state resembling the base environment (Fig. 3, endpoint repeatability index of B1–B6 and S6 = 0.93, *SI Appendix*, Fig. S1).

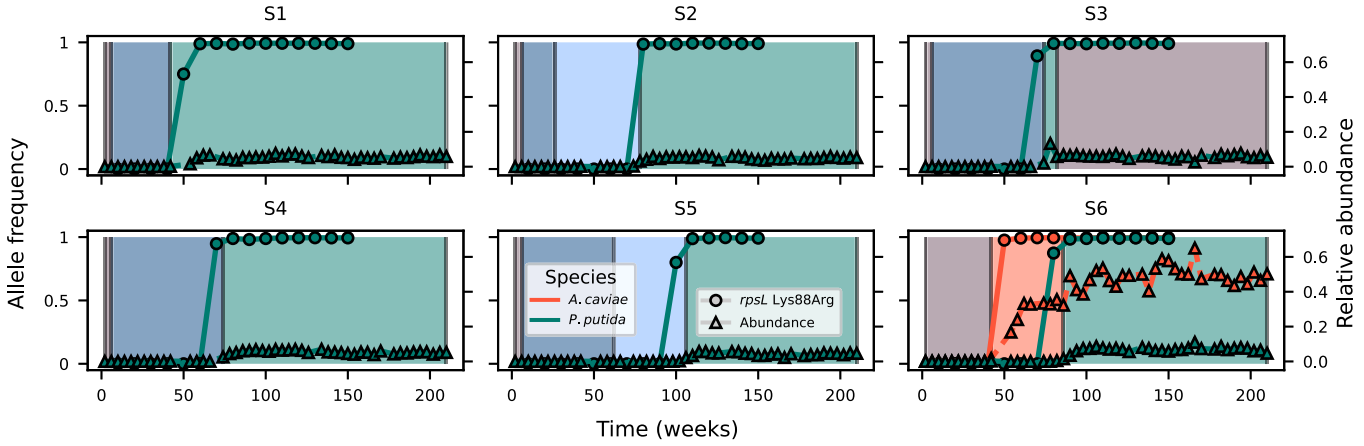

Fig. 4. Selective sweeps of a nonsynonymous point mutation (lysine to arginine in the 88th codon, Lys88Arg) in the gene *rpsL* in *Aeromonas caviae* (orange) and *Pseudomonas putida* (green) are linked to community state shifts (i.e. epoch changes) in the streptomycin community replicates. Solid lines and circles show the allele frequency of the mutation (*Left* y-axis) and the dashed lines with triangles show the relative abundance of the species (*Right* y-axis). The background shows the epochs of Fig. 3.

Resistance Evolution Induced Recurrent State Shifts. An eco-evolutionary feedback drove the state shifts in the streptomycin environment. This feedback arose through selective sweeps of a known streptomycin resistance point mutation in the *rpsL* gene (Lys88Arg, e.g., ref. 34) in *Pseudomonas putida* (S1–S6) and *A. caviae* (S6) detected by metagenome sequencing and validated through clone isolation and growth assays (Fig. 4). These adaptive events not only led to an increase in the species' relative abundances but also reshaped the community structure: *Pseudomonas chlororaphis* decreased as *P. putida* increased, and *A. caviae* increased at the cost of *C. koseri* (Fig. 3). Such shifts align with competitive exclusion among closely related taxa with similar metabolic pathways (29). Together, the results show that evolutionary adaptation in *P. putida* and *A. caviae* reverberated through the community by restructuring ecological interactions.

To test causality, we introduced sensitive and resistant *P. putida* or *A. caviae* clones (24 clones isolated from week 151) to the ancestral communities growing either in the base or streptomycin environment. Resistant clones of both species established successfully in the streptomycin environment and altered community composition whereas sensitive clones did not establish (*SI Appendix*, Figs. S2 and S3). Especially in the streptomycin environment, resistant *A. caviae* shifted the community composition toward that of the base environment (repeatability index = 0.92, *SI Appendix*, Figs. S2 and S3), confirming its role as driver of community composition. These data also show that *P. putida* had higher relative abundance than *P. chlororaphis* in the base environment and in the streptomycin environment if, and only if, a resistant *P. putida* clone was introduced (*SI Appendix*, Fig. S4). As a control, introduction of sensitive or resistant *P. putida* clones did not have an effect in the base environment and introduction of sensitive *P. putida* clones did not have an effect in the streptomycin environment. This outcome aligned with time-resolved community and genomic data (Figs. 3 and 4) which indicated that streptomycin resistance evolution in *P. putida* drove the state shift observed in all six replicates, while that of *A. caviae* explained the unique trajectory of community S6. We next asked whether the long-term communities would respond similarly. After 207 wk, we branched a parallel experiment, identical to the main study, where resistant *A. caviae* was introduced to the six streptomycin communities that had at that point evolved for 207 wk in their growth medium under streptomycin stress. Invasion succeeded in S1–S5 (in S6 it was already present) shifting community compositions toward the S6 state (Fig. 5).

New Community States Were Robust Against Environment Switch. We tested the robustness of the new community states by switching the environment after week 207. Adding streptomycin to base environment communities B1–B6 eradicated *P. putida* and *A. caviae* while favoring *C. koseri* (Fig. 5). This response arose from the streptomycin sensitivity of *P. putida* and *A. caviae*, and the resistance of *C. koseri*. The similarity of outcomes across the replicates supports the conclusion that long-term base communities had converged to highly repeatable states.

By contrast, removing streptomycin from streptomycin adapted communities S1–S5 left their composition unchanged (Fig. 5). In particular, *A. caviae* did not reappear in communities S1–S5 where it was absent or had a very low abundance (below detection threshold) after the streptomycin treatment. Finally, removing streptomycin had no detectable effect on the relative abundance of *A. caviae* in the S6 community or *P. putida* in S1–S6 communities, suggesting that any fitness cost of streptomycin resistance was absent or mitigated. Together, these findings show that eco-evolutionary dynamics can entrench microbial communities in stable states that persist even under reversal of the environment.

Discussion

In this study, the environment (base versus streptomycin) determined the long-term community state (Fig. 3). Trajectories showed a rapid early transition followed by extended periods of stability, reminiscent of single-species LTEE (35, 36). Unexpectedly, in the streptomycin treatment, it was not the antibiotic stress alone but the subsequent evolution of resistance in *A. caviae* and *P. putida* over one to two years that drove the transition to new community states (Fig. 4). Once resistance arose, communities followed either one distinct trajectory (S1–S5) or one resembling the base environment (S6). These states persisted even after antibiotic removal, indicating resilience, and could be reproducibly induced by introducing a resistant *A. caviae* clone (Fig. 5). The response of community composition to the appearance of resistant *A. caviae* was independent

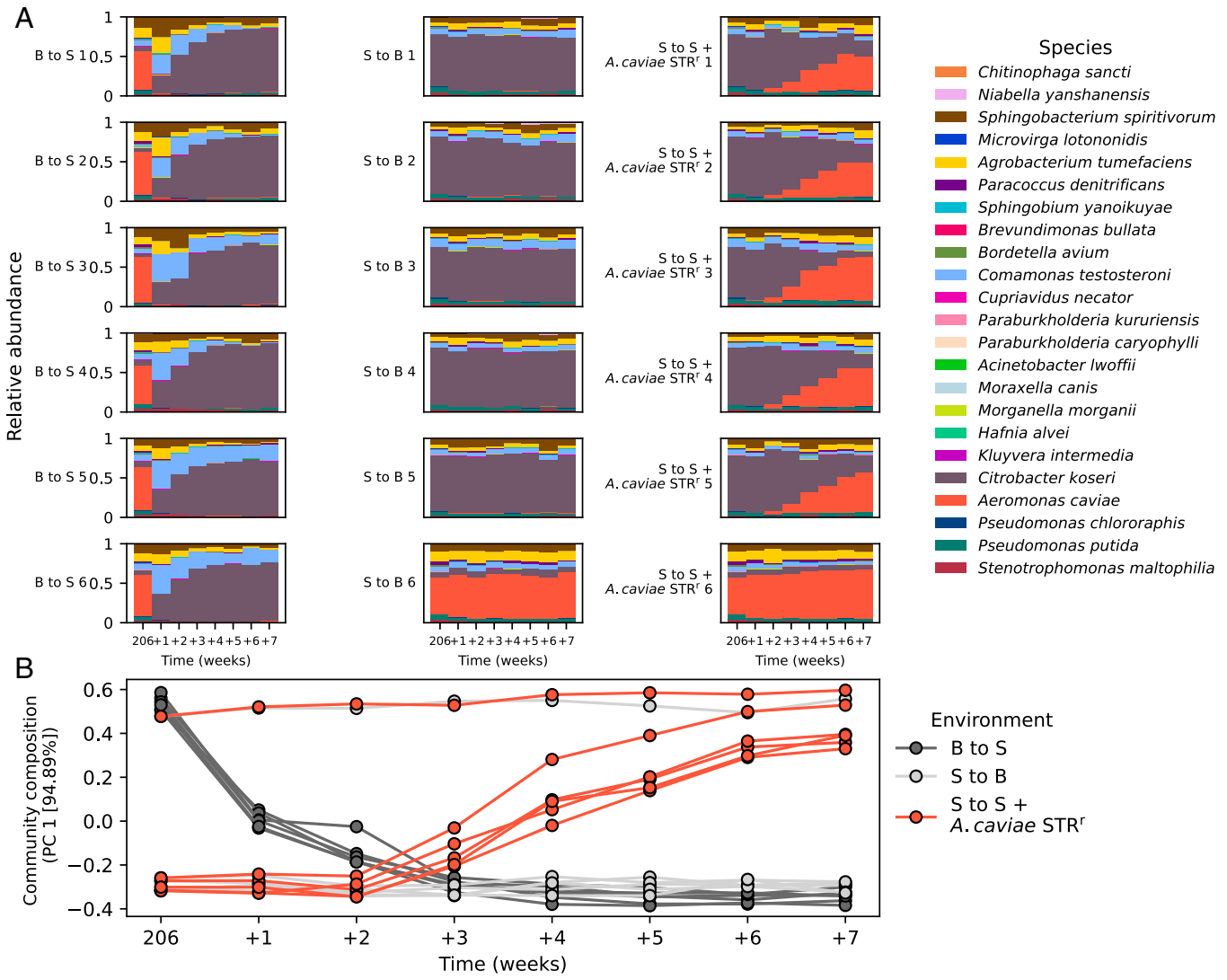

Fig. 5. Consequences of changing the environment (from base, B, to streptomycin, S, or vice versa) or introducing a resistant *A. caviae* clone (STR^r) in streptomycin environment after an evolutionary history of 207 wk. (*A*) The bar charts show the community composition from week 206 in the main experiment to week seven in the validation experiment. (*B*) The scatter plot shows the community composition (principal component 1, PC 1) as a function of time. Each point corresponds to one timepoint in one replicate. Changing the environment of the B communities to streptomycin changed the community structure while the opposite, changing S communities to no streptomycin, did not change the community structure. Resistant *A. caviae* (*A. caviae* STR^r) was able to invade communities S1–S5 where it was absent.

of community history. This suggests that the uniqueness of *A. caviae* resistance evolution in S6 was not due to that particular community but possibly because of its very low population size which limits the chances for mutations. Possible resistance mutations in *rpsL* or *rsmG* genes were detected also in *Agrobacterium tumefaciens*, *Comamonas testosteroni*, *Sphingobacterium spiritivorum*, *Paracoccus denitrificans*, and *P. chlororaphis* (*SI Appendix*, Fig. S5). The first three species are resistant to streptomycin (*SI Appendix*, Table S1) and their resistance mutations did not appear to shape community-level dynamics. Initially sensitive *P. denitrificans* had low prevalence and its resistance evolution did not have a detectable effect on the community dynamics. In case of *P. chlororaphis*, the resistance possibly acquired with the mutations in *rsmG* gene (37) were in some replicates linked with its relative abundance in the streptomycin environment. However, the timing of the mutation and increase in prevalence was not as clear as for *A. caviae* and *P. putida* and more detailed characterization of the mutations and their effect on the community composition would be needed to reveal if the first state shift in replicates S1–S5 were induced by resistance evolution as well.

Evolution was also prevalent in the base environment, with selective sweeps in *Stenotrophomonas maltophilia*, *C. testosteroni*, and *P. denitrificans* (*SI Appendix*, Fig. S5). These within-species evolutionary dynamics together with the low-allele frequency mutations provide interesting avenues for future population genetic studies. However, the timing and length of epochs across base replicates were highly consistent, suggesting that while evolution was common, it caused the community trajectory to diverge from repeatable patterns only with resistance mutations in key taxa. This shows that streptomycin exerts a strong species-specific control on the community and once species resolve the stress they revert the community composition to the nonperturbed state reminiscent of evolutionary rescue.

Twelve of the 23 species had relative abundance of 0 to 5% throughout the experiment. We anticipate that these extinctions, or low abundances, are caused by two things that are not mutually exclusive. The species have different growth characteristics (e.g.

lag time and maximum per capita growth rate) and the species that went extinct are mainly those that grow slowly (*SI Appendix*, Fig. S6). We also expect that there are niche overlaps among the species. In line with this, the phylogenetic diversity is maintained in the community. The 11 species with maximum relative abundance above 5 % represent all phylogenetic classes in the community: *Niabella yanshanensis* (Chitinophagia), *S. spiritivorum* (Sphingobacteriia), *A. tumefaciens* (Alphaproteobacteria), *C. testosteroni* (Betaproteobacteria), *C. koseri*, *A. caviae*, and *P. chlororaphis* (Gammaproteobacteria).

Linking community ecology with population genetics has long been a theoretical goal, yet empirical connections remain scarce. The studies examining the effect of community context on evolution have revealed broad patterns, with mechanisms and species driving changes remaining elusive, e.g., refs. 16, 38, and 39. Here, we directly tested how ecological and evolutionary change interact to shape community dynamics and stability. We show that a de novo mutation in a single key species can redirect the ecological state of an entire microbial community—a striking demonstration of eco-evolutionary feedback dynamics in communities. Contrary to the expectation that antimicrobial resistance carries substantial fitness costs (40), resistant *A. caviae* and *P. putida* produced community-level outcomes comparable to those without streptomycin. This pattern may reflect strong interspecific differences in competitive ability compared to those within species (sensitive versus resistant subclones) or low fitness costs of *rpsL* mutations (41). More broadly, our results demonstrate that evolutionary innovation can reshape community trajectories and reinforce resilience, highlighting how eco-evolutionary dynamics may be harnessed to better understand, predict, and eventually manage the stability of microbial communities in natural and applied settings.

Materials and Methods

Bacteria. The 23 bacterial species forming the synthetic community were from the HAMBI Culture Collection (University of Helsinki). The species were chosen for the community, based on the previous research demonstrating their ability to grow together in mesocosm studies (12, 13, 29). The bacterial species used were *Acinetobacter lwoffii*, *A. caviae*, *A. tumefaciens*, *Brevundimonas bullata*, *Bordetella avium*, *Chitinophaga sancti*, *C. koseri*, *C. testosteroni*, *Cupriavidus necator*, *Hafnia alvei*, *Kluyvera intermedia*, *Microvirga lotononidis*, *Moraxella canis*, *Morganella morganii*, *N. yanshanensis*, *Paraburkholderia caryophylli*, *Paraburkholderia kururiensis*, *P. denitrificans*, *P. chlororaphis*, *P. putida*, *S. spiritivorum*, *Sphingobium yanoikuyae*, and *S. maltophilia* (*SI Appendix*, Table S1).

Long-Term Serial Passage Experiment. Bacterial strains were cultured in 25 ml microcosm flasks that contained 6 ml of 20% Reasoner's 2A (R2A) medium (Neogen). R2A is a low-nutrient medium that hinders the dominance of fast growing species (42) and it has been used in previous studies with this community (12, 13). The experiment consisted of two conditions: base (no streptomycin) and streptomycin environment. The streptomycin concentration in the culture medium was 20 $\mu g \times ml^{-1}$ of streptomycin sulfate and we report the concentration as the concentration of the sulfate. Both environments included six replicate communities. The experiment was initiated by adding a 20 µl mixture of the 23 bacteria species (in equal proportions) to the medium. The flasks were incubated in a shaking cabin at 25 °C for seven days. After seven days, 500 µl of the medium was transferred to a fresh medium as described above. After the seven day growth cycle, the culture was processed as follows: 100 µl culture was collected for measuring optical density (OD) with Absorbance 96 plate reader (Byonoy), two 900 µl culture specimens were pelleted and stored at −20 °C for DNA extraction and sequencing, and 500 µl of culture was frozen with 85 % glycerol (1:1) for further use (e.g. clone isolation). As part of the transfer protocol, the community was reseeded with a tiny amount (less than 1% of the total community biomass) of the ancestral community every sixth transfer. This was done in order to avoid stochastic extinctions during the experiment and to allow evolution via mutations and migration for those species that went extinct or were present at very low abundance.

Short-Term Serial Passage Experiment. The long-term serial passage experiment demonstrated evolution of streptomycin resistance in *P. putida* and *A. caviae*, and community composition changes related to this. These dynamics took years to observe and to assess their repeatability, we performed a 32-d long experiment with serial transfer every 48 h. The same ancestral community, culture medium, and streptomycin concentrations were used as in the long-term experiment. The communities were cultured on 96-well plates in 1 ml volume. As a control, the ancestral 23-species community was grown in streptomycin and streptomycin-free conditions (48 replicates for both conditions). To assess community dynamics related to streptomycin resistance, resistant, or sensitive *A. caviae* and *P. putida* clones, isolated from the long-term experiment (see section below), were introduced to the community. The clone was introduced to the community at the beginning of the experiment, and each clone was introduced to four replicates of the base and streptomycin environments.

Minimum Inhibitory Concentration (MIC) for Streptomycin. Streptomycin sensitivity of the 23 species was assessed by measuring the minimum inhibitory concentrations (MIC). Two replicates of each species were propagated in a monoculture at 25 °C for 48 h and the OD was measured with Bioscreen C (OY Growth Curves Ab Ltd., Finland) using 420 to 580 nm wideband filter. The culture medium was the experiment's base medium (20 % R2A) with streptomycin concentrations of 0, 0.625, 1.25, 2.5, 5, 10, 20, 40, 80, and 160 $\mu g \times ml^{-1}$. MIC was determined as the lowest concentration where the endpoint optical density was below 0.080 for all replicates (*SI Appendix*, Fig. S6 and Table S1).

***Aeromonas caviae* and *Pseudomonas putida* Clone Isolation.** *A. caviae* and *P. putida* clones were isolated from the frozen specimens of the long-term experiment's 151st transfer. Preculture of the frozen pellets was done by incubating them at 25 °C for 24 h in two conditions: 100 % R2A with ampicillin (154 $\mu g \times ml^{-1}$) to enrich *A. caviae* and 100 % R2A with moxifloxacin (0.22 $\mu g \times ml^{-1}$) to enrich *P. putida*. These precultures were diluted to M9 salts and 100 µl of dilution was plated on CHROMagar® Orientation plates. The plates were incubated at 25 °C for 24 h. Colonies of *A. caviae* and *P. putida* were isolated based on their morphology. Isolated colonies were transferred to 100 µl of 100 % R2A, shaked, transferred to 85 % glycerol (1:1) and frozen at −80 °C temperature. Species identification was confirmed with Sanger sequencing. The putatively sensitive clones were those isolated from the base replicates and the putatively resistant clones were those isolated from the streptomycin replicates (resistant *A. caviae* clones present only in replicate S6). The sensitive clones were selected from those that grew in the absence of streptomycin but not at the concentration of 20 $\mu g \times ml^{-1}$, and the resistant clones were selected from those that grew in the absence of streptomycin and at the concentration of 20 $\mu g \times ml^{-1}$ (*SI Appendix*, Fig. S8). Streptomycin MIC was determined with the same protocol as for the ancestral clones of the study species (*SI Appendix*, Fig. S9). Six sensitive and six resistant clones of both species (24 clones in total) were chosen for the experiments. Finally, each selected clone was whole-genome sequenced to confirm that the resistant clones carry the same streptomycin resistance mutation as observed in the long-term experiment, and that the sensitive clones do not carry that mutation (Dataset S6). For the sequencing of the clones, DNA was extracted with DNeasy 96 Blood & Tissue Kit (Qiagen). Sequencing was carried out at SeqCenter (Pittsburgh, Pennsylvania, USA) with the Illumina NovaSeq X Plus sequencer. Clone identifiers and MICs are reported in *SI Appendix*, Table S2.

Validation with Evolved Communities. The short-term serial passage experiment validated the findings in the long-term experiment, namely, that streptomycin affects community composition and that resistance of *A. caviae* or *P. putida* changes it. However, it remained open how a change in the streptomycin condition would affect long-term evolved communities, and if resistant *A. caviae* could invade those five streptomycin communities where it had not evolved streptomycin resistance. To address these questions we performed

an additional serial transfer experiment starting from week 207: Each replicate was transferred to fresh culture medium as usual but an additional transfer was made in the opposite environment, i.e., from base to streptomycin and vice versa. These additional communities were transferred weekly according to the normal transfer protocol and followed for eight weeks by analyzing community composition every week. The second line of validation was to introduce a resistant *A. caviae* clone to the S1–S6 communities to address the question of whether *A. caviae* would become the dominant species also in those communities where it had not evolved resistance during the study period. This was carried out by introducing one of the resistant *A. caviae* clones (clone 3029) used in the other validation experiment to each streptomycin community. These communities were also followed for eight weeks. As control treatments, communities were also maintained in their original environment, and a sensitive *A. caviae* clone (clone 1990) was introduced to S1–S6 communities (*SI Appendix*, Fig. S7). Community composition throughout this experiment was assessed with 16S rRNA gene amplicon sequencing similar to the main study (see below). The 8th timepoint of the experiment had data with suspected errors and was excluded from analyses. In addition, the 3rd time point in S to S replicate 6 was excluded due to a low number of sequencing reads (*SI Appendix*, Fig. S7).

16S rRNA Gene Amplicon Sequencing and Community Composition Analyses. Relative abundances of the 23 species were based on 16S rRNA gene amplicon sequencing. Genomic DNA for community composition analysis was extracted from the frozen sample for every 4th transfer using the DNeasy 96 Blood & Tissue Kit (Qiagen). Sample quality and quantity were assessed using NanoDrop (Thermo Scientific) and Quant-iT 1X dsDNA HS kit (Invitrogen).

Amplicon libraries were constructed following the TaggiMatrix multiplexing procedure (43). Briefly, the V3 region of the 16S rRNA gene was amplified with primers modified to include iTru fusion adapters (Fwd 5′-CCTACGGGAGGCAGCAG-3′, Rev 5′-ATTACCGCGGCTGCTGG-3′) and an internal sample-specific combinatorial index. Amplicons were purified with the NGS Normalization 96-Well Kit (Norgen Biotek), then pooled (96 samples maximum) in a limited-cycle PCR with standard Illumina TruSeq primers and indices. Reaction products were purified with Sera-Mag particles (Cytiva), equimolarly pooled, and the quality of the library was assessed using the Bioanalyzer High sensitivity DNA kit (Agilent). Paired-end sequencing (2 × 150 bp reads) was performed with the Illumina MiSeq 2000 V2 platform at the Finnish Functional Genomics Centre, Turku, Finland. The Illumina BaseSpace software was used to demultiplex the resulting reads on the i5/i7 index pair, producing fastq files that were again demultiplexed on the custom TaggiMatrix index sequences and trimmed of primer sequences using cutadapt (44) version 4.4.

Trimmed and demultiplexed read pairs were merged into a single amplicon using NGmerge (45) version 0.3.0. Quality control was performed using vsearch (46) version 2.22.1 to exclude reads with Ns, more than one expected error, and maximum and minimum lengths greater than or less than 165 and 115 bp, respectively. The reads were assigned to species using Rbec (47) version 1.8.0 with a reference database consisting of unique V3 amplicon sequences from the 23 bacterial species. Amplicon counts were corrected for 16S rRNA gene copy number variation by scaling amplicon counts to the total number of full-length 16S rRNA genes in each genome matching the V3 primer pair (48, 49). Computer code for executing this workflow is available at gitlab.utu.fi/slhogl/hambiAmplicon.

At the beginning the longitudinal 16S rRNA gene data started from the second week and lasted until the 210th transfer, yielding 53 timepoints (one per every fourth week). Of the 53 timepoints, three had missing data (weeks 46, 50, and 70) in multiple samples, and week 174 had clearly deviating data in multiple samples. Week 130 sample was sequenced in a different laboratory and with a slightly different protocol, yielding qualitatively but not quantitatively comparable data. These five time points were excluded and as a result the longitudinal community composition data consisted of 48 timepoints.

Segmentation of Community Composition Into Epochs. The longitudinal data on the community composition were segmented to understand state shifts and succession of the communities. Segmentation was performed in R environment (50) with package dpseg (51) version 0.1.1. The function dpseg in the package was modified to allow segments to have a minimum length of two timepoints (lower limit originally three). Here, Rcpp package (52, 53) version 1.0.14, was used. The scoring matrix for the segmentation was calculated by taking the average community composition for every 2, 3, 4…48 time point long segments and summing up the Kullback–Leibler divergence of the segment average to each time point within the segment. We consider thus identified segments to represent community state epochs.

Repeatability of Community Composition. Repeatability of community composition among replicates was quantified with the repeatability index described by Venkataram and Kryazhimskiy (54). Community similarity metric s between communities i and j at time t was calculated as $s_{ij}(t) = 1 - \frac{d_{ij}(t)}{\sqrt{2}}$, where $d_{ij}(t)$ is the Euclidean distance of the 23 element long community composition vectors at time t. Repeatability indices for the set of replicates were calculated as the mean of the similarity metrics across all pairwise comparisons per time point.

Metagenome Sequencing and Analyses. Evolution, i.e. the emergence of de novo mutations and changes in their frequency, was studied with deep (metagenomic) sequencing, i.e. sequencing the total DNA of the community. For this, DNA was extracted from the samples from every 10th transfer, spanning weeks 10 to 150, yielding 15 timepoints in total. DNA extraction was carried out with DNeasy 96 Blood & Tissue Kit (Qiagen) in 96-well plate format. The concentration of the extracted DNA was inspected with Quant-iT 1X dsDNA HS kit (Invitrogen) and NanoDrop ND-1000 (Thermo Scientific). Extractions of 60 to 400 ng of DNA at 25 to 40 μl volume were delivered to the sequencing facility (Finnish Functional Genomics Centre, Turku, Finland) for specimen preparation and sequencing.

Metagenomic sequencing was carried out as paired-end whole-genome sequencing (2 × 150 bp reads) performed with the Illumina NovaSeq 6000 S4 platform (version 1.5). Adapter trimming was performed at the sequencing facility with bcl2fastq2 conversion software (Illumina). The total number of sequencing reads per sample was ca. 20 million reads.

Prior to read mapping and other bioinformatic analyses, the technical quality of the metagenomic sequencing data was assessed with FASTQC software (55) version 0.11.9. None of the performed tests indicated any technical problems that would have led to discarding of the data.

Read mapping was performed with the BWA-mem algorithm (56). All samples were mapped against a metareference, constructed from the high-quality reference genomes of each 23 species (49) and a ciliate *Tetrahymena thermophila* strain SB210 (57). *T. thermophila* was included in the metareference in order to map possible *Tetrahymena* reads present in other samples of the sequencing batch. Mapped reads were further processed with SAMtools (58) version 1.21 methods sort, fixmate, markdup, and merge, respectively, to prepare alignments for variant calling.

Variant calling was executed per replicate community, providing alignments of each timepoint as one sample. The workflow and analysis steps followed those in Hoffmann et al. (24). Short variants, i.e., single-nucleotide variants (SNV), multinucleotide variants (MNV), and short indels, were called with GATK (59) version 4.5.0.0 tools MUTECT2 and FilterMutectCalls. In FilterMutectCalls, microbial mode (–microbial-mode) was applied. SNVs with filter quality "PASS" were used in further analyses. After this step, clusters of SNVs were identified with the GATK tool VariantFiltration, by defining the number of SNVs that make up a cluster to two (–cluster-size 2) and size of the search window to 35 bp (–cluster-window-size 35). Ten base pair long flanks were added to each SNV to make a list of SNV cluster regions with Bedtools (60) version 2.31.1. VariantFiltration was further used to exclude these regions and putative mobile elements from the list of SNVs. MNVs and indels with filter quality "PASS" and those that were only observations within a 35 bp long window were retained. Finally the effects of SNVs, MNVs, and indels with a minimum mapping depth of 5, were predicted with snpEff (61) version 4.3t based on gene annotations from Cairns et al. (13). Mutations in protein coding genes, annotated as "CDS," were used in the analysis of evolutionary changes.

Analysis and Interpretation. Downstream analyses and visualization of the data, e.g., community composition and identified mutations were carried out in

Python 3.10 environment using the libraries Numpy (62) version 1.26.4, Scipy (63) version 1.13.0, Seaborn (64) version 0.13.2, pandas (65, 66) version 2.2.2, Matplotlib (67) version 3.8.4, and Scikit-learn (68) version 1.4.2.

Data, Materials, and Software Availability. Sequencing data (fastq read files) are available in ENA under project PRJEB98480 (69). VCF files of the mutation data as well as computer code to reproduce the figures in the main text are available in an Open Science Framework repository at osf.io/7djpk (70). All other data are included in the manuscript and/or supporting information.

ACKNOWLEDGMENTS. We want to acknowledge Meri Lindqvist and Katja Salminen at the Center of Evolutionary Applications (University of Turku), Elisa Zakharova, Ida-Marija Hyvönen, Beda Anttila, Tiia Korpi, Olli Pitkänen, Inga-Katariina Aapalampi, Milla Similä, Atte Aapalampi, Ida Aarni, Trine Link, Emmi Hirvonen, Julia Saloranta, Hilla Pellikka, Linda Nevala, Fanny Koskela, and Irma Warinowski for contribution to the laboratory work. Anthony Sun, Eva Kisdi, and Seppe Kuehn are thanked for discussions. Mikhail Shubin is thanked for his assistance with drawing Fig. 1. This study was supported by Finnish Functional Genomics Centre, University of Turku, and Åbo Akademi and Biocenter Finland. We wish to acknowledge CSC–IT Center for Science, Finland, for computational resources.

Author affiliations: [a]Department of Computer Science, University of Helsinki, Helsinki 00014, Finland; [b]Department of Organismal and Evolutionary Biology, University of Helsinki, Helsinki 00014, Finland; [c]Turku Collegium for Science, Medicine and Technology, University of Turku, Turku 20014, Finland; [d]Department of Biology, University of Turku, Turku 20014, Finland; and [e]Aquatic Ecology and Evolution, Department of Biology, University of Konstanz, Konstanz 78464, Germany

1. D. R. Nemergut *et al*., Patterns and processes of microbial community assembly. *Microbiol. Mol. Biol. Rev.* **77**, 342–356 (2013).
2. M. Scheffer, S. H. Hosper, M. L. Meijer, B. Moss, E. Jeppesen, Alternative equilibria in shallow lakes. *Trends Ecol. Evol.* **8**, 275–279 (1993).
3. M. F. De La Cochetière *et al*., Resilience of the dominant human fecal microbiota upon short-course antibiotic challenge. *J. Clin. Microbiol.* **43**, 5588–5592 (2005).
4. C. Y. Chang, D. Bajić, J. C. C. Vila, S. Estrela, A. Sanchez, Emergent coexistence in multispecies microbial communities. *Sci. N. Y.* **381**, 343–348 (2023).
5. J. Friedman, L. M. Higgins, J. Gore, Community structure follows simple assembly rules in microbial microcosms. *Nat. Ecol. Evol.* **1**, 109 (2017).
6. B. H. Good, M. J. McDonald, J. E. Barrick, R. E. Lenski, M. M. Desai, The dynamics of molecular evolution over 60,000 generations. *Nature* **551**, 45–50 (2017).
7. P. J. Gerrish, R. E. Lenski, The fate of competing beneficial mutations in an asexual population. *Genetica* **102–103**, 127–144 (1998).
8. M. Łuksza, M. Lässig, A predictive fitness model for influenza. *Nature* **507**, 57–61 (2014).
9. M. Lässig, V. Mustonen, A. M. Walczak, Predicting evolution. *Nat. Ecol. Evol.* **1**, 77 (2017).
10. M. Meijers, D. Ruchnewitz, J. Eberhardt, M. Łuksza, M. Lässig, Population immunity predicts evolutionary trajectories of SARS-CoV-2. *Cell* **186**, 5151–5164.e13 (2023).
11. M. J. Bottery *et al*., Inter-species interactions alter antibiotic efficacy in bacterial communities. *ISME J.* **16**, 812–821 (2022).
12. J. Cairns, R. Jokela, L. Becks, V. Mustonen, T. Hiltunen, Repeatable ecological dynamics govern the response of experimental communities to antibiotic pulse perturbation. *Nat. Ecol. Evol.* **4**, 1385–1394 (2020).
13. J. Cairns, S. Hogle, E. Alitupa, V. Mustonen, T. Hiltunen, Pre-exposure of abundant species to disturbance improves resilience in microbial metacommunities. *Nat. Ecol. Evol.* **9**, 395–405 (2025).
14. E. Hesse *et al*., Parallel ecological and evolutionary responses to selection in a natural bacterial community. *Proc. Natl. Acad. Sci. U.S.A.* **121**, e2403577121 (2024).
15. L. D. Potts *et al*., Chronic environmental perturbation influences microbial community assembly patterns. *Environ. Sci. Technol.* **56**, 2300–2311 (2022).
16. B. H. Good, L. B. Rosenfeld, Eco-evolutionary feedbacks in the human gut microbiome. *Nat. Commun.* **14**, 7146 (2023).
17. T. G. Barraclough, How do species interactions affect evolutionary dynamics across whole communities? *Annu. Rev. Ecol. Evol. Syst.* **46**, 25–48 (2015).
18. T. W. Schoener, The newest synthesis: Understanding the interplay of evolutionary and ecological dynamics. *Sci. N. Y.* **331**, 426–429 (2011).
19. J. A. Ascensao, M. M. Desai, Experimental evolution in an era of molecular manipulation. *Nat. Rev. Genet.* **27**, 81–95 (2025).
20. E. T. Granato, T. A. Meiller-Legrand, K. R. Foster, The evolution and ecology of bacterial warfare. *Curr. Biol.* **29**, R521–R537 (2019).
21. J. A. Ascensao, K. M. Wetmore, B. H. Good, A. P. Arkin, O. Hallatschek, Quantifying the local adaptive landscape of a nascent bacterial community. *Nat. Commun.* **14**, 248 (2023).
22. L. Leónidas Cardoso, P. Durão, M. Amicone, I. Gordo, Dysbiosis individualizes the fitness effect of antibiotic resistance in the mammalian gut. *Nat. Ecol. Evol.* **4**, 1268–1278 (2020).
23. P. Fang, A. X. Elena, M. A. Kunath, T. U. Berendonk, U. Klümper, Reduced selection for antibiotic resistance in community context is maintained despite pressure by additional antibiotics. *ISME Commun.* **3**, 52 (2023).
24. J. Hoffmann, S. Hogle, T. Hiltunen, L. Becks, Temporal changes in the role of species sorting and evolution determine community dynamics. *Ecol. Lett.* **28**, e70033 (2025).
25. D. Lawrence *et al*., Species interactions alter evolutionary responses to a novel environment. *PLoS Biol.* **10**, e1001330 (2012).
26. G. Martin, T. Lenormand, The fitness effect of mutations across environments: Fisher's geometrical model with multiple optima. *Evol. Int. J. Org. Evol.* **69**, 1433–1447 (2015).
27. S. Muzafar, R. R. Nair, D. I. Andersson, O. M. Warsi, The strength of interspecies interaction in a microbial community determines its susceptibility to invasion. *PLoS Biol.* **22**, e3002889 (2024).
28. R. R. Nair, D. I. Andersson, Interspecies interaction reduces selection for antibiotic resistance in *Escherichia coli*. *Commun. Biol.* **6**, 331 (2023).
29. J. Cairns *et al*., Construction and characterization of synthetic bacterial community for experimental ecology and evolution. *Front. Genet.* **9**, 312 (2018).
30. H. Celiker, J. Gore, Clustering in community structure across replicate ecosystems following a long-term bacterial evolution experiment. *Nat. Commun.* **5**, 4643 (2014).
31. N. Meroz, N. Tovi, Y. Sorokin, J. Friedman, Community composition of microbial microcosms follows simple assembly rules at evolutionary timescales. *Nat. Commun.* **12**, 2891 (2021).
32. N. Meroz *et al*., Evolution in microbial microcosms is highly parallel, regardless of the presence of interacting species. *Cell Syst.* **15**, 930–940.e5 (2024).
33. A. Pascual-García, D. W. Rivett, M. L. Jones, T. Bell, Replicating community dynamics reveals how initial composition shapes the functional outcomes of bacterial communities. *Nat. Commun.* **16**, 3002 (2025).
34. S. T. Gregory, J. H. Cate, A. E. Dahlberg, Streptomycin-resistant and streptomycin-dependent mutants of the extreme thermophile *Thermus thermophilus*. *J. Mol. Biol.* **309**, 333–338 (2001).
35. R. E. Lenski, M. R. Rose, S. C. Simpson, S. C. Tadler, Long-term experimental evolution in *Escherichia coli*. I. Adaptation and divergence during 2,000 generations. *Am. Natural.* **138**, 1315–1341 (1991).
36. R. E. Lenski, M. Travisano, Dynamics of adaptation and diversification: A 10,000-generation experiment with bacterial populations. *Proc. Natl. Acad. Sci. U.S.A.* **91**, 6808–6814 (1994).
37. K. Nishimura, T. Hosaka, S. Tokuyama, S. Okamoto, K. Ochi, Mutations in *rsmG*, encoding a 16S rRNA methyltransferase, result in low-level streptomycin resistance and antibiotic overproduction in *Streptomyces coelicolor* A3(2). *J. Bacteriol.* **189**, 3876–3883 (2007).
38. U. Klümper *et al*., Selection for antimicrobial resistance is reduced when embedded in a natural microbial community. *ISME J.* **13**, 2927–2937 (2019).
39. T. Scheuerl *et al*., Bacterial adaptation is constrained in complex communities. *Nat. Commun.* **11**, 754 (2020).
40. D. I. Andersson, D. Hughes, Antibiotic resistance and its cost: Is it possible to reverse resistance? *Nat. Rev. Microbiol.* **8**, 260–271 (2010).
41. D. I. Andersson, B. R. Levin, The biological cost of antibiotic resistance. *Curr. Opin. Microbiol.* **2**, 489–493 (1999).
42. D. J. Reasoner, E. E. Geldreich, A new medium for the enumeration and subculture of bacteria from potable water. *Appl. Environ. Microbiol.* **49**, 1–7 (1985).
43. T. C. Glenn *et al*., Adapterama II: Universal amplicon sequencing on Illumina platforms (TaggiMatrix). *PeerJ* **7**, e7786 (2019).
44. M. Martin, Cutadapt removes adapter sequences from high-throughput sequencing reads. *EMBnet. J.* **17**, 10–12 (2011).
45. J. M. Gaspar, NGmerge: Merging paired-end reads via novel empirically-derived models of sequencing errors. *BMC Bioinf.* **19**, 536 (2018).
46. T. Rognes, T. Flouri, B. Nichols, C. Quince, F. Mahé, VSEARCH: A versatile open source tool for metagenomics. *PeerJ* **4**, e2584 (2016).
47. P. Zhang, S. Spaepen, Y. Bai, S. Hacquard, R. Garrido-Oter, Rbec: A tool for analysis of amplicon sequencing data from synthetic microbial communities. *ISME Commun.* **1**, 73 (2021).
48. S. L. Hogle *et al*., Effects of phenotypic variation on consumer coexistence and prey community structure. *Ecol. Lett.* **25**, 307–319 (2022).
49. S. L. Hogle, M. Tamminen, T. Hiltunen, Complete genome sequences of 30 bacterial species from a synthetic community. *Microbiol. Resour. Announc.* **13**, e0011124 (2024).
50. R Core Team, R: A language and environment for statistical computing (R version 4.5.2, Vienna, Austria, 2025).
51. R. Machne, P. F. Stadler, dpseg: Piecewise linear segmentation by dynamic programming (R package Version 0.1.1, CRAN, 2020).
52. D. Eddelbuettel, R. François, Rcpp: Seamless R and C++ integration *J. Stat. Softw.* **40**, i08 (2011).
53. D. Eddelbuettel *et al*., Rcpp: Seamless R and C++ integration (R package Version 1.1.0, CRAN, 2025).
54. S. Venkataram, S. Kryazhimskiy, Evolutionary repeatability of emergent properties of ecological communities. *Philos. Trans. R. Soc. Lond. Ser. B Biol. Sci.* **378**, 20220047 (2023).
55. S. Andrews, FastQC: A quality control tool for high throughput sequence data (2019). https://www.bioinformatics.babraham.ac.uk/projects/fastqc/. Accessed 9 October 2025.
56. H. Li, Aligning sequence reads, clone sequences and assembly contigs with BWA-MEM. arXiv [Preprint] (2013). https://doi.org/10.48550/arXiv.1303.3997 (Accessed 9 October 2025).
57. J. A. Eisen *et al*., Macronuclear genome sequence of the ciliate *Tetrahymena thermophila*, a model eukaryote. *PLoS Biol.* **4**, e286 (2006).
58. P. Danecek *et al*., Twelve years of SAMtools and BCFtools. *GigaScience* **10**, giab008 (2021).
59. G. A. Van der Auwera, B. D. O'connor, *Genomics Cloud: Using Docker, GATK, and WDL in Terra* (O'Reilly Media, ed. 1, 2020).
60. A. R. Quinlan, I. M. Hall, BEDTools: A flexible suite of utilities for comparing genomic features. *Bioinf. (Oxford, England)* **26**, 841–842 (2010).
61. P. Cingolani *et al*., A program for annotating and predicting the effects of single nucleotide polymorphisms, SnpEff: SNPs in the genome of *Drosophila melanogaster* strain w1118; iso-2; iso-3. *Fly* **6**, 80–92 (2012).
62. C. R. Harris *et al*., Array programming with NumPy. *Nature* **585**, 357–362 (2020).
63. P. Virtanen *et al*., SciPy 1.0: Fundamental algorithms for scientific computing in Python. *Nat. Methods* **17**, 261–272 (2020).
64. M. Waskom, seaborn: Statistical data visualization. *J. Open Sour. Soft.* **6**, 3021 (2021).
65. W. McKinney, "Data structures for statistical computing in Python" in *Proceedings of the 9th Python in Science Conference*, S. van der Walt, J. Millman, Eds. (SciPy, 2010), pp. 56–61.

66. The Pandas Development Team, pandas-dev/pandas: Pandas. Zenodo. https://doi.org/10.5281/zenodo.10957263. Accessed 9 October 2025.
67. J. D. Hunter, Matplotlib: A 2D graphics environment. *Comput. Sci. Eng.* **9**, 90–95 (2007).
68. F. Pedregosa *et al.*, Machine learning in Python. *J. Mach. Learn. Res.* **12**, 2825–2830 (2011).
69. M. Kivikoski *et al.*, PRJEB98480 Long-term microbial community experiment. European Nucleotide Archive (ENA). https://www.ebi.ac.uk/ena/browser/view/PRJEB98480. Deposited 26 March 2026.
70. M. Kivikoski *et al.*, Supporting material to "Evolution induced state shifts in a long-term microbial community experiment." Open Science Framework. https://osf.io/7djpk/. Deposited 30 March 2026.